Journal of Engineering Science and Technology
Vol. XX, No. Y (Year) PPP - QQQ

A NOVEL METHOD TO OPTIMIZE THE POWER UTILIZATION OF SINGLE FLUID HEAT TRANSFER SYSTEM

PRANAVANAND SATYAMURTHY*, RAGHURAM A.

Dept. of EIE, VNR Vignana Jyothi Institute of Engg. and Tech, Hyderabad, India
Dept. of EEE, JNTUH College of Engineering, Hyderabad, India
*Corresponding Author: pranavanand_s@vnrvjiet.in

Abstract

In this paper, a Novel Hybrid control approach is applied to a Single Fluid Heat Transfer System. Mathematical model of the system has been developed. The proposed control scheme can reduce the power burn rate by 21%. The Novel Hybrid controller is robust against perturbations. The control scheme has been corroborated on the numerical simulations. The transient response attributes have been used as validating strictures.

Keywords:Single Fluid Heat Transfer System, LabVIEW, Power utilizations optimization, Nonlinear controller, Hybrid controller.

1. Introduction

Off late, due to simple operational procedure and easy maintenance, SFHTS finds pinnacle position in the process industries. SFHTS is a nonlinear system. In this project, mathematical model of the process has been developed. The Sliding Mode and Feedback Linearization Controllers have better efficacy to control the nonlinear process than the linear controllers. The Fuzzy-PID control scheme yields less effective control on the nonlinear system than the Sliding Mode control scheme [1]. The chattering problem associated with the Sliding mode controller is solved by increasing the dynamics of the controller [2]. An additional compensator resulted in a modified Sliding Mode controller that performed better than the classical controllers [3]. Feedback Linearization controller and Sliding Mode controller can handle the nonlinearities better than the PID controller [4]. Development of Higher Order Sliding Mode Controller is computationally exhaustive process. The Feedback Linearization (FL) controller is used as an effective replacement to Higher Order Sliding Mode Controller [5]. Feedback

Nomenclatures

A	Area of cross section of the flow tube, m^2
B_s	Positive scalar
C_{pc}	Specific heat of the liquid, J/kgK
h_d	Delivery head, m
h_s	Suction head, m
P_h	Hydraulic power, W
P_s	Pump shaft power, W
s_n	Time variables, s
S_s	Positive scalar
T_{ci}	Inlet temperature of Theminol-D12, K
T_{co}	Outlet temperature of Theminol-D12, K
T_{hi}	Inlet steam temperature, K
T_{hsp}	Set Point during heating operation, K
T_{csp}	Set Point during cooling operation, K
U	Heat transfer coefficient , W/m^2K
V_C	Volume of the cold liquid, m^3
V_H	Volume of the hot liquid, m^3
v_c	Volumetric flow rate of cold liquid, m^3/s
v_h	Volumetric flow rate of hot liquid, m^3/s

Greek Symbols

ŋ	Positive value
η	Pump efficiency
Π	Control strategy
τ^2	Lyapunov type function
ρ_c	Density of the liquid, kg/m^3.
ψ_n	$'s_n$

Abbreviations

PID	Proportional Integral Derivative
NHB	Novel Hybrid
SFHTS	Single Fluid Heat Transfer System
SM	Sliding Mode

Linearization Controller provides better control than the conventional linear controllers [6]. The Feedback Linearization can replace the numerical equations derived from kinetics of the system [7]. It's computationally less complex too [8].

2. Block diagram and explanation of SFHTS

The Block diagram of SFHTS is shown in Fig. 1. The Therminol-D12 is the thermal agent that heats or cools the Chemical/Mass in the inner tank of the Concentric Jacket Tank. The outer tank of the Concentric Jacket tank is filled with Therminol-D12 to desired/set level. Therminol-D12 is heated or cooled to transfer the thermal energy to the Chemical/Mass in the inner tank. To control the

flow of Therminol-D12 from Concentric Jacket Tank to Expansion Tank, a manually operated ball valve is used. In the proposed mechanical design, the manually operated ball valve is removed and a single controller is used to control the level in both the tanks.

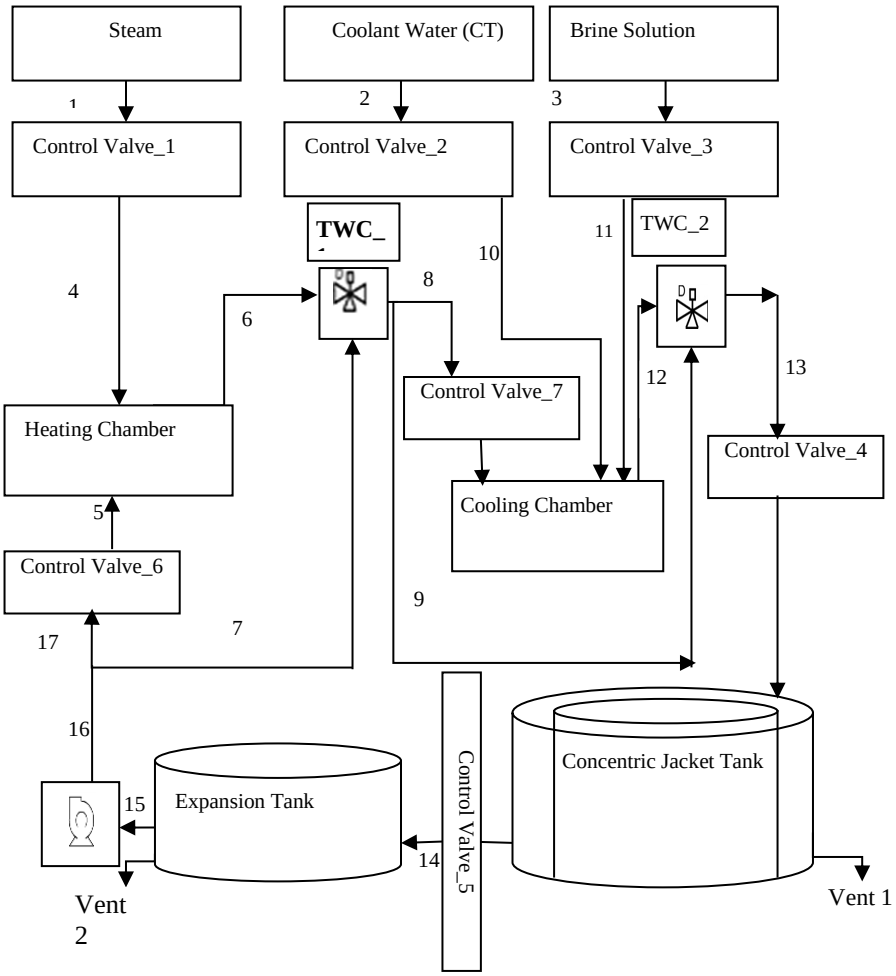

Fig. 1. Block Diagram of the process.

2.1. Heating process

Therminol–D12 is drawn from the Expansion Tank (Storage Tank) by the pump via the pipe (15). Therminol-D12 is allowed to flow through heating chamber via pipe(5). During the heating process the cooling chamber is manually put in off position. Simultaneously, Therminol-D12 flows to pipe (7), which is attached to the TWC_1. At any instant, the TWC_1 allows flow from either terminal 1 or terminal 3 but not both. Hence the pipe (7) throughput, which is coupled to 3rd terminal of Three-way control valve (TWC_1), is blocked and Therminol-D12 flows through pipe (5) alone. The heating chamber has steam supply via Control valve_1, pipe (1) and Therminol-D12 via pipe (5). The heat is transferred from

Steam to Therminol-D12. Here the heat transfer takes place by non-contact conduction method. The heated Therminol-D12 is delivered via pipe (6) to TWC_1 which allows the Therminol-D12 to flow through it. The output from the TWC_1 is allowed to flow through pipe (9). The pipe (8) is connected to the cooling chamber. In the SFHTS, at any instant, either heating or cooling can take place but not both. Hence the cooling chamber is manually put in off condition during heating. Control Valve_7 blocks the flow of Therminol-D12. This arrangement makes Therminol-D12 to flow through pipe (9) to TWC_2's 3rd terminal. The 3rd terminal is allowed to access the TWC_2's output and hence Therminol-D12 flows to Concentric Jacket Tank via pipe (3) and Control Valve_4. The level of Therminol-D12 is maintained at a pre-set level in the Concentric Jacket Tank. The piping arrangement to perform one heating cycle is 16-17-15-Control Valve_6-5-6-9-13-Control Valve_5-14. Therminol-D12 then flows back to the Expansion Tank. The process is repeated till the desired temperature of Therminol-D12 is attained.

2.2. Cooling process

During the cooling process, the heating chamber is manually put in off condition. The TWC_1's 3rd terminal is open and Therminol-D12 flows via pipe (7) to pipe (8). The entire Therminol-D12 flows to the cooling chamber via Control Valve_7. The cooling chamber has two source of coolants: Coolant Water (CT) and Brine Solution. Depending upon the requirement, either the Coolant Water or Brine Solution is allowed to flow via their respective control valves, 2 and 3. The output of the cooling chamber is connected to TWC_2's 1st terminal via pipe (12). The TWC_2 gives access of its output to 1st terminal. Theminol-D12 flows to Concentric Jacket Tank via pipe (13) and Control Valve_4. The piping arrangement for cooling cycle is 16-7-8-12-13-13-Control Valve_5-14. The process is repeated till the process variable reach the desired set point.

2.3. Mathematical model

The state space model of the system is written as

$\dot{x} = A(x) + Bu$

$y = C(x) + Du$

'$\dot{x}$' and *'y'* represents the state equation and output equation respectively. '*A*' represents state matrix, '*B*' represents input matrix, '*C*' represents output matrix and '*D*' represents feedforward/ disturbance/feedthrough matrix [9]. This equation represents a LTI system [10]. But, the SFHTS is a nonlinear system. Hence, the state space model of the nonlinear system is represented by a bilinear state space model [11] and written as

$$\dot{x} = \begin{bmatrix} \frac{-UA}{C_{pc}\rho_c V_c} & \frac{UA}{C_{pc}\rho_c V_c} \\ \frac{UA}{C_{ph}\rho_h V_h} & -\frac{UA}{C_{ph}\rho_h V_h} \end{bmatrix} x + \begin{bmatrix} \frac{T_{ci}}{V_c} - \frac{1}{V_c}x_1 & 0 \\ 0 & \frac{T_{hi}}{V_h} - \frac{1}{V_h}x_2 \end{bmatrix} u \quad (1)$$

$$\begin{bmatrix} x_1 \\ x_2 \end{bmatrix} = \begin{bmatrix} T_{co} \\ T_{ho} \end{bmatrix} \quad (2)$$

$y = x\,; u = \begin{bmatrix} v_c \\ v_h \end{bmatrix};\ u_1 = v_c \text{ and } u_2 = v_h$

with $x, u, y \in R^2$ being a two-dimension vector [12].

As per the dynamics of the system, the rate of change of temperature is directly proportional to (i) the ratio of volumetric flow rate to the volume of the liquid to be heated times the difference between the outlet and inlet temperature, (ii) the area of heat exchanger (A) times the heat transfer coefficient of the liquid (U), (iii) the steam inlet and Therminol-D12 outlet temperature, (iv) difference between the set point and process variable temperature and inversely proportional to product of specific heat, density and volume of the liquid to be heated [13].

Let, $a_1 = \frac{UA}{C_{pc}\rho_c V_c}$ *and* $a_2 = \frac{UA}{C_{ph}\rho_h V_h}$

The above state space equation is written as,

$$\dot{x}_1 = -a_1 x_1 + a_1 x_2 + \left\{\frac{T_{ci}}{V_c} - \frac{x_1}{V_c}\right\} u_1 \quad (3)$$

$$\dot{x}_2 = a_2 x_1 - a_2 x_2 + \left\{\frac{T_{hi}}{V_h} - \frac{x_2}{V_h}\right\} u_2 \quad (4)$$

Let,

$$g_o(x) = f(x) = \begin{bmatrix} -a_1 x_1 + a_1 x_2 \\ a_2 x_2 - a_2 x_2 \end{bmatrix};\ g_1(x) = \begin{bmatrix} \frac{T_{ci}}{V_c} - \frac{x_1}{V_c} \\ 0 \end{bmatrix};\ g_2(x) = \begin{bmatrix} 0 \\ \frac{T_{hi}}{V_h} - \frac{x_2}{V_h} \end{bmatrix}$$

The above equation is written as

$$\dot{x} = Ax + \sum_{i=1}^{n} N_i x u_i + Bu \quad (5)$$

with 'N' the bilinear state convention term originating from output convention [14] and

$N_1 = \begin{bmatrix} \frac{-1}{V_c} & 0 \\ 0 & 0 \end{bmatrix}, N_2 = \begin{bmatrix} 0 & 0 \\ 0 & \frac{-1}{V_h} \end{bmatrix}$ and the input term originating from the input convention with, $B = \begin{bmatrix} \frac{T_{ci}}{V_c} & 0 \\ 0 & \frac{T_{hi}}{V_h} \end{bmatrix}$

In all the equations, the 't' term is intentionally suppressed for easy computation.

Units Confirmation:

$$\dot{x}_1 = -a_1 x_1 + a_1 x_2 + \left\{\frac{T_{ci}}{V_c} - \frac{x_1}{V_c}\right\} u_1$$

$$a_1 x_1 = \frac{-UA}{C_{pc}\rho_c V_c} x_1 = \frac{\frac{W}{m^2 K} m^2 ℃}{\frac{J}{KgK} * \frac{Kg}{m^3} * m^3} = \frac{W℃}{KJ}.$$

As, W = kJ/s so the unit is $\frac{℃}{s}$

Similarly, for $a_1 x_2 = \frac{℃}{s}$.

The third summative term of the equation has the following variables. T_{ci} and x_1 are the temperature variables, V_c is the volume in m^3 and u_1 is the flow rate in m^3/s. Substituting the units for these variables yields $^oC/s$ and is demonstrated below.

$$\left\{\frac{T_{ci}}{V_c} - \frac{x_1}{V_c}\right\} u_1 = \left\{\frac{℃}{m^3} - \frac{℃}{m^3}\right\} * \frac{m^3}{s} = \frac{℃}{s} \quad (6)$$

All the summative terms of the equation represent the same unit (rate of change of temperature).

3. Controller development: Validation and Verification

3.1. NHB controller for heating operation

A computationally less exhaustive NHB controller has been developed with good robustness and perturbation rejection capability.

The dynamic model of the thermal transfer system is written as [15],

$$\dot{x} = Ax + \sum_{i=1}^{n} N_i x u_i + Bu$$

$$\dot{x}_1 = -a_1 x_1 + a_1 x_2 + \left\{\frac{T_{ci}}{V_c} - \frac{x_1}{V_c}\right\} u_1$$

$$\dot{x}_2 = a_2 x_1 - a_2 x_2 + \left\{\frac{T_{hi}}{V_h} - \frac{x_2}{V_h}\right\} u_2$$

The controller accelerates the rate of change of temperature for large magnitude differences between Set Point and Process Variable (temperature). The acceleration reduces as the process variables approaches the set temperature. When the process variable exceeds the set temperature, the polarity of the controller changes and brings the process variable to the set value [16]. When the set point is reached, the manipulated variable maintains status quo.

Let $\Omega_1 = \frac{1}{s_1} \neq 0$ and $\Omega_2 = \frac{1}{s_2} \neq 0$, where s_1 and s_2 are the time variables in seconds with $s_1 > s_2$. So, $\Omega_1 < \Omega_2$

The controller is derived as,

$$u_1 = -\frac{1}{\frac{T_{ci}}{V_c} - \frac{x_1}{V_c}}\left\{-a_1 x_1 + a_1 x_2 + \Omega_1 x_1 + \Omega_2 (T_{co} - T_{hsp})\right\} \quad (7)$$

When, T_{co} reaches T_{hsp} and remains constant for a sampling period then $\dot{x}_1 = 0$. The status quo of u_1 is maintained. When, $T_{co} > T_{hsp}$, then $\dot{x}_1$ tends to be negative magnitude and hence the flow rate is manipulated to make process variable reach the set point, that is, $T_{co} = T_{hsp}$ and preserve $\dot{x}_1$ at 0. When, $T_{co} < T_{hsp}$, then $\dot{x}_1$ tends to be positive magnitude and hence flow rate is manipulated to make $T_{co} = T_{hsp}$ and maintain $\dot{x}_1$ at 0. The controller brought the system to the set point and guaranteed asymptotic stability.

A switching surface is defined with S_s being a positive scalar. When the flow rate is disturbed, then "u_1" is disturbed. So, the controller developed should provide negation against flow disturbance. Hence, a new control strategy is developed imbibing the present state of flow rate.

$$\Pi = g + \frac{1}{\frac{T_{ci}}{V_c} - \frac{x_1}{V_c}}\left\{-a_1 x_1 + a_1 x_2 + \Omega_1 x_1 + \Omega_2 (T_{co} - T_{hsp})\right\} \quad (8)$$

where "g" indicates the present flow rate.

Differentiating Π with respect to time,

$$\frac{d}{dt}(\Pi) = \dot{\Pi} = \frac{d}{dt}\left\{g + \frac{1}{\frac{T_{ci}}{V_c} - \frac{x_1}{V_c}}\left\{-a_1 x_1 + a_1 x_2 + \Omega_1 x_1 + \Omega_2 (T_{co} - T_{hsp})\right\}\right\}$$

$$\Rightarrow \dot{g} + \frac{d}{dt}\left\{\frac{1}{\frac{T_{ci}}{V_c} - \frac{x_1}{V_c}}\{-a_1x_1 + a_1x_2 + \Omega_1x_1 + \Omega_2(T_{co} - T_{hsp})\}\right\}$$

Let $\dot{g} = u_1$. To maintain stability and to reject disturbance, the controller should bring the flow rate to previous stable state. If 'Δ' is the increase in the flow rate from the previous immediate equilibrium state then the controller should decrement the flow rate by an appropriate quantity and vice versa. The controller

$$u_1 = -S_s\, Sign\,(\Pi) - Sign\left\{\frac{d}{dt}\left\{\frac{1}{\frac{T_{ci}}{V_c} - \frac{x_1}{V_c}}\{-a_1x_1 + a_1x_2 + \Omega_1x_1 + \Omega_2(T_{co} - T_{hsp})\}\right\}\right\}$$
$$* \frac{d}{dt}\left\{\frac{1}{\frac{T_{ci}}{V_c} - \frac{x_1}{V_c}}\{-a_1x_1 + a_1x_2 + \Omega_1x_1 + \Omega_2(T_{co} - T_{hsp})\}\right\}$$

achieves the said goal. Upon substituting the value for $\dot{\Pi}$, $\dot{\Pi} = -S_s\, Sign\,(\Pi)$. When, $T_{co} = T_{hsp}$, x_1 is constant and hence $\dot{x_1} = 0$. When g is varied then, $T_{co} - T_{hsp}$, may either become positive or negative and the controller brings the system back to the desired state, that is, $T_{co} = T_{hsp}$ .The controller has the dynamics to bring the system back to the state prior to the perturbation. Also, the reachability component of the controller is confirmed as it satisfies the condition, $\frac{1}{2}\frac{d}{dt}\Pi^2 \leq \eta|s|$, where Π^2 is Lyapunov type function [17]. It is further proved that $\Pi\dot{\Pi} < \eta|s|$ where, η is small positive value such that $0 \leq \eta \leq 5$. The controller satisfies the finite time reachability and stability conditions.

3.2. NHB controller for cooling operation

The dynamics of the cooling system is given as

$$\dot{x}_2 = -a_2x_2 + a_2x_1 + \left\{\frac{T_{hi}}{V_h} - \frac{x_2}{V_h}\right\}u_2$$

Let $\psi_1 = \frac{1}{s_1} \neq 0$ and $\psi_2 = \frac{1}{s_2} \neq 0$ where s_1 and s_2 are the time variables in seconds with $s_1 > s_2$. So, $\psi_1 < \psi_2$

The controller,

$$u_2 = -\frac{1}{\frac{T_{hi}}{V_h} - \frac{x_2}{V_h}}\{-a_2x_2 + a_2x_1 + \psi_1x_1 + \psi_2(T_{ho} - T_{csp})\}$$

brings the system to the set point and guarantees asymptotic stability. A switching surface is defined with B_s being a positive scalar.

Let, $\tau = h + \frac{1}{\frac{T_{hi}}{V_h} - \frac{x_2}{V_h}}\{-a_2x_2 + a_2x_1 + \psi_1x_1 + \psi_2(T_{ho} - T_{csp})\}$ (9)

where "h" indicates the present flow rate.

Differentiating τ with respect to time,

$$\frac{d}{dt}(\tau) = \dot{\tau} = \frac{d}{dt}\left\{ h + \frac{1}{\frac{T_{hi}}{V_h} - \frac{x_2}{V_h}}\{-a_2x_2 + a_2x_1 + \psi_1x_1 + \psi_2(T_{ho} - T_{csp})\}\right\}$$

$$\Rightarrow \dot{h} + \frac{d}{dt}\left\{\frac{1}{\frac{T_{hi}}{V_h} - \frac{x_2}{V_h}}\{-a_2x_2 + a_2x_1 + \psi_1x_1 + \psi_2(T_{ho} - T_{csp})\}\right\}$$

where, $\dot{h} = \dot{u_2}$, the rate of change of flow rate.

$$\dot{u_2} = -S_s\, Sign\,(\tau) - Sign\left\{\frac{d}{dt}\left\{\frac{1}{\frac{T_{hi}}{V_h} - \frac{x_2}{V_h}}\{-a_2x_2 + a_2x_1 + \psi_1x_1 + \psi_2(T_{ho} - T_{csp})\}\right\}\right\}$$

$$* \frac{d}{dt}\left\{\frac{1}{\frac{T_{hi}}{V_h} - \frac{x_2}{V_h}}\{-a_2x_2 + a_2x_1 + \psi_1x_1 + \psi_2(T_{ho} - T_{csp})\}\right\}$$

has the dynamics to bring the system back to the state prior to perturbation.

The reachability component of the controller is confirmed by satisfying the condition, $\frac{1}{2}\frac{d}{dt}\tau^2 \leq \eta|s|$, where τ^2 is Lyapunov type function [17]. It is further proved that $\tau\dot{\tau} < \eta|s|$ where η is small positive value such that $0 \leq \eta \leq 5$. The controller designed satisfies the finite time reachability and stability conditions [17].

3.3. Power utilization optimization

The ideal hydraulic power required to drive a pump depends on the mass flow rate, the liquid density and the differential height. Based on "The National Certification Examinations for Energy Managers and Energy Auditors" guide book, and [18], the Hydraulic Power,

P_h = Q($\frac{m^3}{s}$) x Total head,$(h_d - h_s)$ (m) x ρ(kg/m^3) x g (m/s^2) / 1000

where h_d- Discharge head, h_s-Suction head, ρ - Density of the fluid and
g - Acceleration due to gravity.

The Pump shaft power (P_s) = Hydraulic power (P_h) / pump efficiency (η_{Pump}).

The Electrical input power = $\frac{\text{Pump shaft power}}{\eta\, motor}$.

The pump is operated to deliver Therminol-D12 at the flow rate of 20 m^3/hour.

3.4. Hydraulic power calculation

The following are the parameters considered for Power calculation.

1. Flow rate of Therminol-D12 = 20 m^3/ hour or 0.0055 m^3/ s
2. Density of Therminol-D12 = 756 Kg/m^3
3. Difference between suction head and discharge head = 3 m

4. Acceleration due to gravity = 9.81 m/s^2

The pump and motor efficiency are assumed as 90 %.

Hydraulic Power = .0055×3×756×9.81/1000 = 0 .12 kW

Pump shaft power (P_s) = Hydraulic power (P_h)/ pump efficiency (η *Pump*)
= 0.12/ .90 = 0.13 kW

Electrical input power = $\frac{\text{Pump shaft power}}{\eta \text{ motor}}$ = 0.13 / .90 = 0.14 kW

The NHB controller facilitated the process variable to reach the set point by operating the pump to deliver Therminol-D12 at 15±0.5 m^3/ hour. Hence, the flow rate of 15 m^3/ hour or 0.0041$\frac{m^3}{s}$ considered for further calculations. So,

P_h = 0.0041×3×756×9.81 / 1000 = 0.09 kW

P_s= 0.09/ .90 = 0.1 kW

Electrical input power = 0.1 / .90 = 0.11kW

Percentage decrease in power consumption = (0.14-0.11/0.14)×100 = 21.4 %

Hence, by running the pump at an optimal speed to deliver Therminol-D12 at 15 $m^3/hour$, power consumed by the pump is reduced by 21.4%.

4. Results and Discussion

Thermal Energy Transfer module is a nonlinear batch process. As per the industry requirement the process variable should reach the set temperature, generally ±10℃ more than the present or current temperature, of Thermionol-D12 in 600 seconds at a minimum ramp rate of $1℃/minute$. The controller should help the process variable to reach the set point in stipulated time.

The results below present the efficacy of different controllers in reaching the set point and negating the perturbation. The system was subjected to perturbation at 720th second. From Figs. 2, 3 and 4 it is evident that the SM and NHB controller insulated the system from perturbation. They have the efficacy to negate the perturbation effect.

To have a holistic view of the process, three desired temperatures 20°C, 60°C and 90°C are set, covering the complete spectrum of operation. The following are the inferences.

PID and PI controllers couldn't elude the overshoot effect and the system's response to both the controllers is identical.

The SM controller eliminated the overshoot. The gain of the SM controller has been compromised to shun the chattering effect. The values obtained from the graphs are shown in Table 1.

NHB controller eliminated the overshoot effect, attained faster settling time with no chattering effect. It is also inferred from the quantified values that the dynamics of the system is faster at higher set temperatures. Based on the above quantified result, NHB controller is recommended for the heating operation of Thermal energy transfer module.

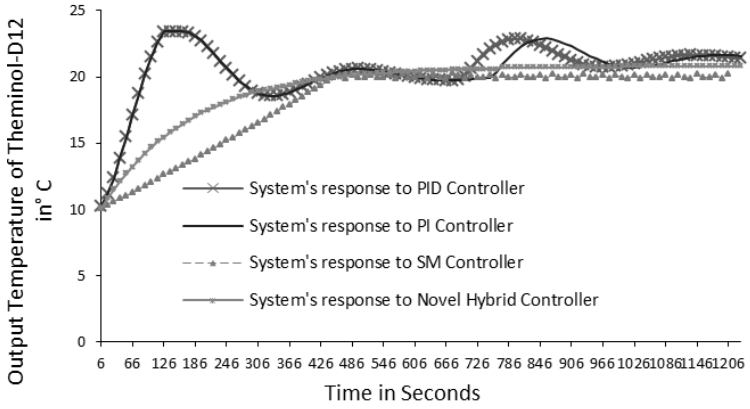

Fig. 2. System's response to different controllers with set point 20 ° C.

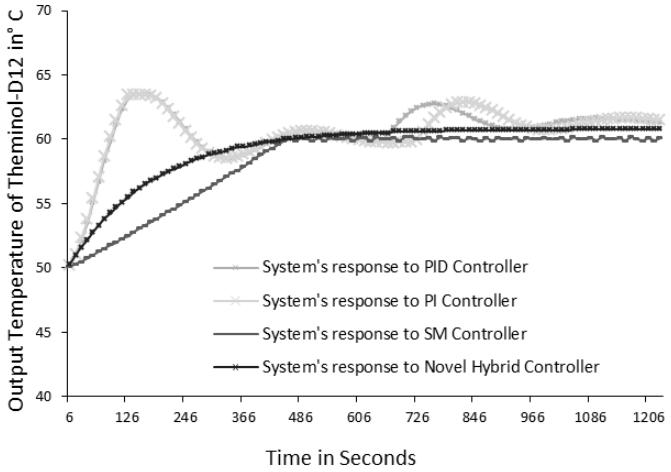

Fig. 3. System's response to different controllers with set point 60 ° C.

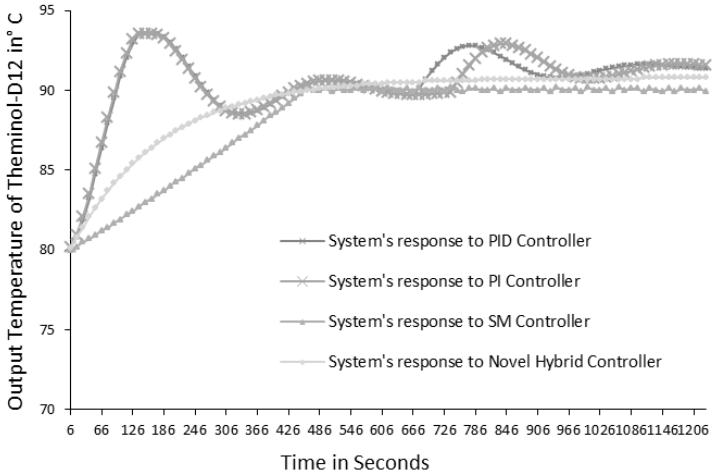

Fig. 4. System's response to different controllers with set point 90 ° C.

Table 1. Inference from Figs. 2, 3 and 4.

Controller	Set Point (°C)	Inlet Temperature of Process Variable (°C)	Overshoot (%)	Approximate Settling time (Seconds)	Approximate Rise time (Seconds)
PID	20	10	30	400	100
PI	20	10	30	400	100
SM	20	10	Nil	400	280
NHB	20	10	Nil	300	280
PID	60	50	30	350	90
PI	60	50	30	350	90
SM	60	50	Nil	350	300
NHB	60	50	Nil	300	250
PID	90	80	30	300	80
PI	90	80	30	300	80
SM	90	80	Nil	300	300
NHB	90	80	Nil	280	250

Moreover, when the system is subjected to intentional flow disturbance at 720^{th} second, the linear controllers could not retain the process variable at its set point. However, the NHB controlled triumphed in this attribute too.

Figure 5 shows the manipulated variable (flow rate) values for different controllers and set points. Table 2 gives the details of maximum and minimum flow rate when the system was controlled by different controllers. It is observed from the flow rate graph that all the controllers guided the system to reach their respective set point at flow rate of 15 ± 0.5 m^3/ hour. The pump is operated to deliver Therminol-D12 at the aforesaid flow rate and the power consumed is reduced by 21.5%.

The flow rate graph is plotted for three set points and four controllers considered in this project. It is observed that the flow rate of Therminol-D12 increased from the initial flow rate. As per the system dynamics, when the inlet steam temperature and the pressure is maintained constant, the flow rate is directly proportional to the temperature change.

When the system was controller by PID Controller, the flow rate increased steeply from 0 m^3/hour to 20 m^3/hour . The control valve opened linearly from its initial value to maximum value within two and half minutes. The control law again forced the control valve to ebb its opening from 170^{th} - 180^{th} seconds onwards till 300^{th} - 310^{th} seconds. Eventually, the flow rate decreased from 20 m^3/hour to approximately 13 m^3/hour.

Table 2. Inference from Fig. 5.

Parameter (Flow rate)	Controller			
	PID	**PI**	**SM**	**NHB**
Maximum	20	20	16	15
Minimum	0	0	0	0

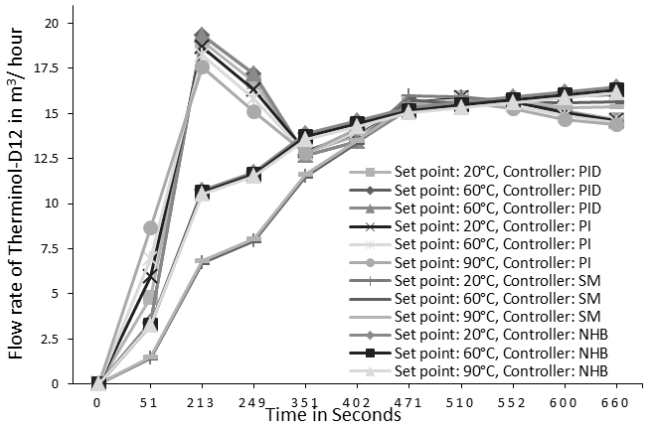

Fig. 5. Flow rate for different set points and controllers.

At approximately 310th second, the control law augmented the valve opening and increased the flow rate to 16.5 m^3/hour. Again, the control valve manipulated to recede the valve opening and reduce the flow rate to 14 m^3/hour before finally settling to 15 m^3/hour at 500th second. It is observed that the control valve is subjected to oscillatory motion of low frequency.

When the system was controller by PI Controller, the dynamics stated above followed but for the swiftness. Again, it is observed that the control valve was subjected to oscillation of low frequency. On comparison with the PID controller, the stress on the control valve is reduced.

To optimally reach the set temperature, the control valve is subjected to oscillatory input. This subside the sensitivity, fidelity and lead to premature failure of the control valve.

When the system was controller by SM Controller, the flow rate increased linearly from 0 m^3/hour at 0th second to 16 m^3/hour at 450th second and settled. The gain of the SM controller has been abated to reduce the chattering effect.

When the system was controller by NHB Controller, the flow rate increased linearly from 0 m^3/hour at 0th second to 16 m^3/hour at 450th second and settled. The control valve was not subjected to oscillatory input. But this phenomenon is evident in PID and PI Controllers controlled process. Even though, low in amplitude and frequency, more than one hundred number of operation cycles is executed per day. Hence, this oscillation leaves its footprint on the performance of the control valve. Similar is the case for cooling operation too.

To have a holistic view of the process, three desired points, 10°C, 50°C and 80°C has been set covering the spectrum of operation. Figs. 6, 7 and 8 portrays the system's response to different controllers. Figure 9 portrays the flow rate of the above system. The parameters considered for evaluating the performance of the controllers are quantified in Table 3 and the maximum and minimum flow rate has been quantified in Table 4.

The PID and PI controllers did not subside the overshoot effect in the system. The SM controller eliminated the overshoot effect in the system. The gain of the SM

controller was reduced to avoid chattering effect and hence resulted in longer settling time. When NHB controller was implemented on the system, the set point was reached in shorter period with no overshoot and chattering. Hence, NHB controller is recommended for the cooling operation of Thermal energy transfer module.

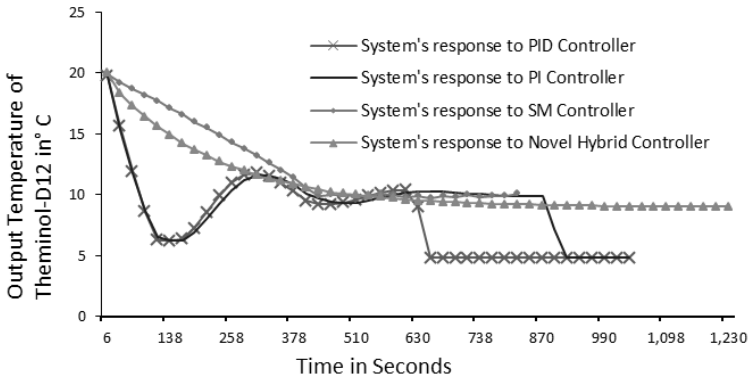

Fig. 6. System's response to different controllers with set point, 10 ° C.

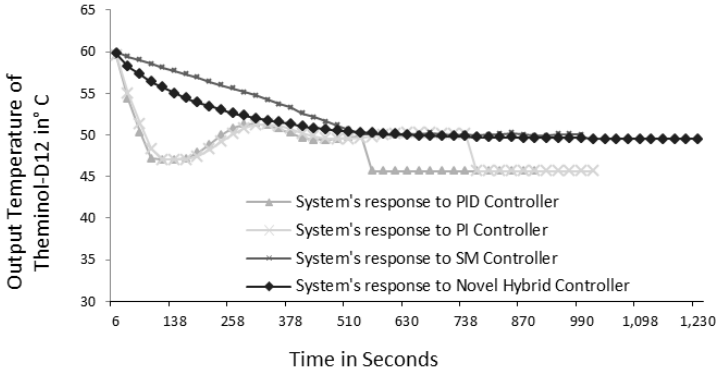

Fig. 7. System's response to different controllers with set point, 50 ° C.

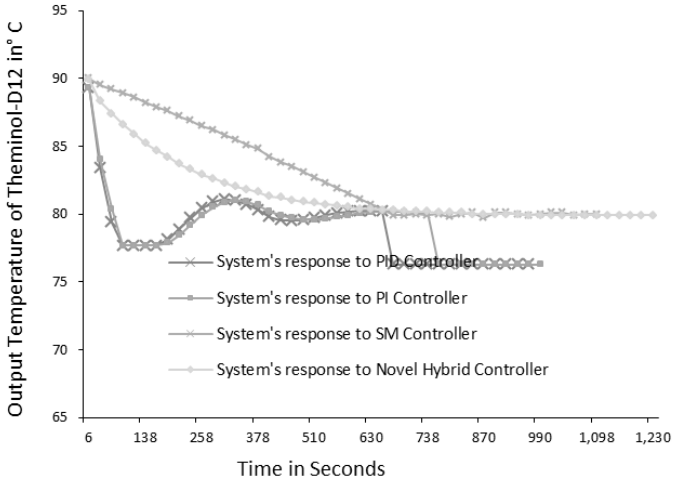

Fig. 8. System's response to different controllers with set point, 80 °C.

Table 3. Inference from Figs. 6, 7 and 8.

Controller	Set Point (°C)	Inlet Temperature of Process Variable (°C)	Overshoot (%)	Approximate Settling time (Seconds)	Approximate Rise time (Seconds)
PID	10	20	40	500	110
PI	10	20	40	520	110
SM	10	20	Nil	440	420
NHB	10	20	Nil	430	410
PID	50	60	30	440	100
PI	50	60	30	440	110
SM	50	60	Nil	410	390
NHB	50	60	Nil	350	306
PID	80	90	20	510	90
PI	80	90	20	510	90
SM	80	90	Nil	600	550
NHB	80	90	Nil	450	400

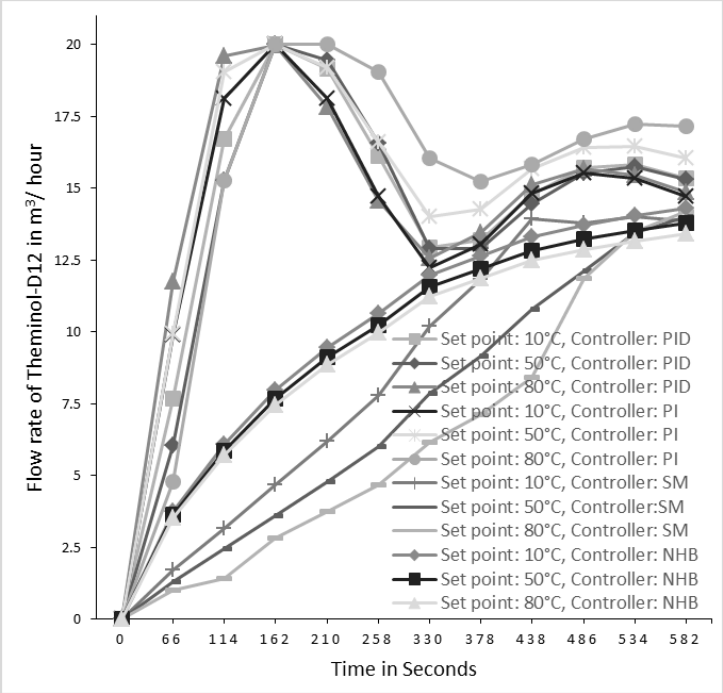

Fig. 9. Flow rate for different set points and controllers.

Table 4. Inference from Fig. 9.

Parameter (Flow rate in m^3/ hour)	Controller PID	PI	SM	NHB
Maximum	20	20	16	15
Minimum	0	0	0	0

5. Conclusions

In summary, it is observed that by operating the pump to deliver Therminol-D12 at a flow rate of 15 m^3/ hour, the set point has been reached. Approximately, 21.5% of power consumed by the pump is reduced by running the pump to deliver Therminol-D12 at 15 ± 0.5 m^3/ hour. When PID, PI and SM controllers were used to control the system, the control valve is stressed. Hence, based on the merits to reduce power consumption, to reach the set temperature faster with no overshoot and to optimize the control valve life and efficiency, NHB controller is recommended for SFHTS. The mechanical design modification reduced the human intervention by eliminating the ball valve between the tanks and enabled a single controller to control the level of Therminol-D12 in both the tanks instead of two controllers.

References

1. Antonella, F.; and Matteo, R. (2009). A sub-optimal second order sliding mode controller for systems with saturating actuators. *IEEE Transactions on Automatic Control*, 54 (5), 1082-1087.
2. Jeang-Lin, C. (2013). Dynamic compensator-based second-order sliding mode controller design for mechanical systems. *IET Control Theory Application*, 7 (13), 1675-1682.
3. Daniel, G.M.; Carlos, R.; and Roberto, G. (2016). Improved design of sliding-mode controllers based on the requirements of MPPT techniques, *IEEE Transactions on Power Electronics*, 31(1), 235-246.
4. Akshaya, M.; and Dash, P.K. (2010). Input-output linearization and robust sliding-mode controller for the VSC-HVDC transmission link. *IEEE Transactions on Power Delivery*, 25(3), 1952-1961.
5. Curtis, D.J. (2006). *Process control instrumentation* (8th ed.). New Delhi: Prentice Hall of India Pvt Ltd.
6. Diogo, R.; Billeter, J.; and Bonvin, D. (2015). Control of reaction systems via rate estimation and feedback linearization. *Computer Aided Chemical Engineering*, 37, 137-142.
7. Sekhar, P.C.; and Mishra, S. (2014). Sliding mode based feedback linearizing controller for grid connected multiple fuel cells scenario. *International Journal of Electrical Power & Energy Systems*, 60, 190-202.
8. Innocenti, G.; and Paoletti, P. (2014). on the robustness of feedback linearization of lur'e systems. *Procedia Engineering*, 79, 407-410
9. Hangos, K.M.; Bokor, J.; and Szederkenyi, G. (2004). *Analysis and control of Nonlinear Process systems (2nd ed.).* London: Springer-Verlag.
10. Jean, J.; Slotine, E.; and Weiping, L. (1991). *Applied nonlinear control (3rd ed.).* New Jersey: Prentice Hall International.
11. Hai, W.; Zhihong-Man.; Do-Manh, T.; Zhenwei, C.; and Weixiang, Shen. (2014). Sliding Mode Control for Steer-by-Wire Systems with AC Motors in Road Vehicles. *IEEE transactions on Industrial Electronics*, 61(3), 1596-1611.

12. Reham, H.; Angel, C. P.; Abdelali, E. A.; and Luis, M. S. (2014). Synthesis of canonical elements for power processing in dc distribution systems using cascaded converters and sliding-mode control. *IEEE Transactions on Power Electronics*, 29 (3), 1366-1380.
13. Naif, B. A.; and Mohamed, Z. (2016). *Sliding mode controllers for a tempered glass furnace*. ISA Transactions, 60, 21-37.
14. Jian-Xin, X.; Zhao-Qin, G.; and Tong, H.; Lee, V. (2014). Design and implementation of integral sliding-mode control on an underactuated two-wheeled mobile robot. *IEEE Transactions on Industrial Electronics*, 61(7), 3671-3681.
15. Eastop, T.D.; and McConkey, A. (2012). *Applied thermodynamics for engineering technologist* (3rd ed.). New Delhi: Pearson Education.
16. Ricardo de, C.; RuiEsteves, A.; and Diamantino, F. (2013). Wheel slip control of evs based on sliding mode technique with conditional integrators. *IEEE Transactions on Industrial Electronics*, 60 (8), 3256-3271.
17. Günyaz, A. (2015). Variable structure controllers for unstable processes. *Journal of Process Control*, 32, 10-15.
18. Albert, T.; and William, J.Y. (2003). *Handbook of energy audit* (2nd ed.). GA, The Fairmont Press.